Stochastically Induced Coherence in Bistable Systems

Andrew J. Irwin, Simon J. Fraser, and Raymond Kapral
Chemical Physics Theory Group, Department of Chemistry, University of Toronto, Toronto, Ontario, Canada M5S 1A1
(Received 14 November 1989)

A new type of resonance phenomenon in a class of bistable oscillators driven by a periodic dichotomous noise process is described. The phenomenon manifests itself as troughs or peaks in the stationary density and has its origin in the appearance of periodic orbits in the noisy dynamics. The stationary density exhibits many self-similar scaling features as the system parameters are tuned, and these features are discussed. Since the noise process is easy to implement and the phenomenon is quite general, it should be possible to observe such resonances in experiments.

PACS numbers: 05.40.+j, 02.50.+s, 05.45.+b, 46.10.+z

Stochastically forced bistable oscillators underlie the description of a wide range of physical phenomena related to internally or externally induced transition rate processes between two deterministically stable states.[1] The equation of motion for the "coordinate" q of such a system is

$$m\ddot{q} = -\zeta\dot{q} + F(q,a(t)), \tag{1}$$

where $F(q,a(t))$ is a general force term that depends on the stochastic process $a(t)$, and ζ is the friction coefficient. The stochastic process in (1) may be additive, multiplicative, or both. Electrical, optical, and mechanical systems may oscillate, whereas chemical rate laws for systems with a single intermediate correspond to an overdamped version of (1); the "mass" m controls this effect.

We focus on a particular stochastic process that produces random changes in the potential function that governs the oscillator dynamics. More specifically, we consider the *periodic dichotomous* noise process $a(t)$ defined in the following way: After lapses of fixed duration τ, $a(t)$ takes the values a_0 with probability p or a_1 with probability $1-p$. For this noise process, (1) corresponds to jumping randomly at intervals τ between potentials $V_i(q) = V(q,a_i)$, with $i=0,1$, where $F(q,a_i) = -dV_i(q)/dq$. The bistable potential $V_i(q)$ can be parametrized so that V_0 and V_1 correspond to cases where the right or left potential well is destroyed and transitions between these regions occur as a result of random changes in the potential function. This periodic dichotomous noise process leads to a new class of phenomena which we term *stochastically induced coherence* —structured spires or troughs in the stationary probability density; it arises from the interplay between the bistability in the average potential and the fixed switching time τ, and is amenable to experimental test. We first discuss the nature of the phenomena and then describe how experiments may be designed to test the predictions of the theory.

By considering a quadratic approximation about each minimum in the bistable potential we obtain a model that is analytically tractable and yet illustrates all the essential features of stochastically induced coherence. Since the dynamics is globally linear for each quadratic potential, we can construct an explicit diffeomorphism for each branch of the potential in terms of the system parameters and the lapse time τ. Much of the dynamics of this solvable example underlies that of more complex bistable potentials. Dividing by the mass and introducing the linear force, (1) becomes

$$\ddot{q} = -\gamma\dot{q} - \omega^2 q + \omega^2/2 + a_i(t), \tag{2}$$

where ω is the oscillator frequency, $\gamma = \zeta/m$, and $a_{0,1} = \mp\omega^2/2$. The indices $i=0,1$ now refer to the locations of the minima of the two quadratic potentials. Introducing the phase-space variables q and $\dot{q}=v$, (2) can be written as a pair of first-order equations and integrated over the time interval τ to yield the pair of 2D maps,

$$\begin{aligned} q(t+1) &= \alpha_+ q(t) + \mu v(t) + (1-\alpha_+)\xi(t), \\ v(t+1) &= -\omega^2\mu q(t) + \alpha_- v(t) + \omega^2\mu\xi(t), \end{aligned} \tag{3}$$

where the Boolean random variable $\xi(t)$ is 0 with probability p and 1 with probability $1-p$, t is measured in units of τ, and

$$\alpha_\pm\Delta\omega = \omega_+ e^{\omega_\mp\tau} - \omega_- e^{\omega_\pm\tau}, \quad \mu\Delta\omega = e^{\omega_+\tau} - e^{\omega_-\tau}.$$

Here $\omega_\pm = -\gamma/2 \pm [(\gamma/2)^2 - \omega^2]^{1/2}$ and $\Delta\omega = \omega_+ - \omega_-$. When $\xi = i$ the map (3) will be called map M_i. Letting $\mathbf{r}$ be the phase point (q,v), we have $M_i\mathbf{r} = \mathbf{r}_i'$. Either branch M_i is a nonsymmetry linear 2D map with a single fixed-point attractor and global behavior ranging from oscillations in the underdamped regime to monotone behavior in the overdamped regime. While the dynamics on each branch is trivial, definite sequences in the stochastic forcing can lead to periodic orbits which give rise to the stochastically induced coherence.

Consider the overdamped regime. Apart from a shift of origin, each branch M_i of the stochastic map is a contraction with the same real eigenvalues $\lambda_\pm = \exp(\omega_\pm\tau)$ and right $|i_\pm\rangle$ and left $\langle i_\pm|$ eigenvectors, so the maps

are conjugate under a translation of origin. The eigenvectors associated with each origin are parallel and, suitably normalized, form the sides of a parallelogram. For overdamped dynamics, once the phase points enter this parallelogram they are trapped. In terms of the eigenvectors of the M_0 branch, we may write $\mathbf{r}=c_+|0_+\rangle+c_-|0_-\rangle$, and using the spectral representations of M_i in the M_0 basis we have for $i=0,1$

$$M_{i,\pm}:\ c'_{i,\pm}=i(1-\lambda_\pm)+\lambda_\pm c_\pm\,. \tag{4}$$

Hence, in this representation the pair of 2D maps M_i reduces to two separate $(\pm)$ pairs of 1D maps $M_{i,\pm}$. Both $\pm$ trajectories are coded by the same stochastic map sequence. The eigenvalues $\lambda_\pm$ can be made to vary such that $0\le\lambda_-\le\lambda_+\le 1$. Therefore we now focus on the 1D case and to simplify the notation the branches f_i are defined by

$$f_i:\ x'_i=i(1-\lambda)+\lambda x\quad(i=0,1)\,, \tag{5}$$

where the eigenvalue λ is the contraction parameter and x is the fractional distance along the corresponding side (eigendirection) of the parallelogram.

The branches of (5) define the stochastic difference equation

$$x(t+1)=\lambda x(t)+(1-\lambda)\xi(t)\,, \tag{6}$$

where $\xi(t)$ is the Boolean random variable defined in (3). At any λ, the invariant density of the stochastic process (6) can be obtained from a single trajectory. Figure 1 shows the λ dependence of this density for $p=\frac{1}{2}$ in the λ-x plane. Evidently, the invariant density is organized by two infinite sets of lines that emerge from $x=0$ and $x=1$ at $\lambda=0$. Lines in one set only cross lines in the other, so for $\lambda<\frac{1}{2}$ there are no crossings giving a gap-filled structure. For $\lambda>\frac{1}{2}$ most of the interval is accessible; a conspicuous latticelike region of crossings near $\lambda=\frac{1}{2}$ changes abruptly, at $\lambda=(\sqrt{5}-1)/2$, into a region of smooth density at larger λ. We now discuss the distinctive behavior in these three regimes, and the singular behavior at the parameter points that separate them.

Cantor set regime.—For $\lambda\in(0,\frac{1}{2})$, the invariant density is a Cantor set. Under f_0 the interval $[0,1]$ is mapped into $[0,\lambda]$, while under f_1 it is mapped into $[1-\lambda,1]$. For $\lambda<\frac{1}{2}$ these intervals are disjoint with an intervening gap. Successive iterations of the map produce a hierarchy of nested, disjoint intervals whose limit is a Cantor set with scaling length λ, so the fractal dimension[2] D is $-\log 2/\log\lambda$. At $\lambda=0$, $D=0$ because the Cantor set has collapsed onto the end points $x=0$ and $x=1$, and at $\lambda=\frac{1}{2}$, $D=1$ because it fills the unit interval.

Resonance regime.—For $\lambda\in[\frac{1}{2},(\sqrt{5}-1)/2]$, the crossing sets of lines produce self-similar bands in the invariant density. It is useful to consider the stationary solutions ρ^* to the Chapman-Kolmogorov equation corresponding to (6):

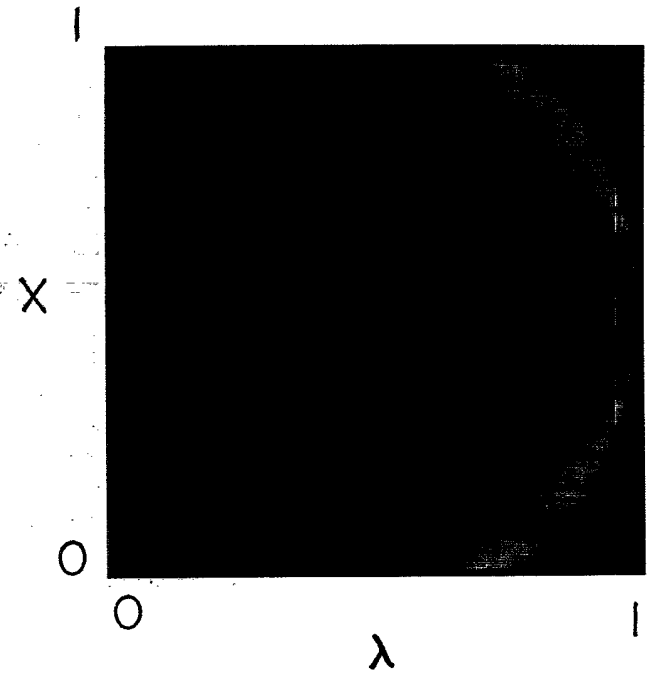

FIG. 1. Stationary density ρ^* in the λ-x plane. High-density regions are blue and low-density regions are red.

$$\rho(x,t+1)=\lambda^{-1}\{p\rho(x/\lambda,t)+(1-p)\rho((x+\lambda-1)/\lambda,t)\}\,, \tag{7}$$

which must be solved subject to the condition that $\rho^*(x)=0$ for $x\notin[0,1]$. The spectrum of (7) lies in the open unit disk, apart from eigenvalue 1 for ρ^*, so this stationary density can be found by iteration. However, we can also find ρ^* explicitly at some λ; e.g., at $\lambda=\frac{1}{2}$ where crossing first occurs the density is uniform for $p=\frac{1}{2}$.

For all values of $\lambda>\frac{1}{2}$ the support[2] of ρ^* is $[0,1]$ (but ρ^* may vanish on a dense set). For λ just above $\frac{1}{2}$, Fig. 1 shows structured high-density (blue) wedges corresponding to flat-topped peaks; as λ increases these merge into regions of low-density (red) wedges which we term trough resonances. The most intense of these occurs at $\lambda=(\sqrt{5}-1)/2$. For larger λ there are only faint structures, and these seem to disappear above $\lambda=1/\sqrt{2}$. The origin of these resonances is not difficult to understand. We first examine the nature of the envelope of ρ^* near the end points 0 and 1. The integral of $\rho^*(x)$ over an interval $[0,x]$ is the distribution function or mass on that interval $m^*(0,x)$, say. For ρ^*, Eq. (7) then yields

$$m^*(0,x)=pm^*(0,x/\lambda)+(1-p)m^*(0,(x+\lambda-1)/\lambda)\,. \tag{8}$$

If x is chosen such that $x<1-\lambda$, which is true suffi-

are conjugate under a translation of origin. The eigenvectors associated with each origin are parallel and, suitably normalized, form the sides of a parallelogram. For overdamped dynamics, once the phase points enter this parallelogram they are trapped. In terms of the eigenvectors of the M_0 branch, we may write $\mathbf{r}=c_+|0_+\rangle+c_-|0_-\rangle$, and using the spectral representations of M_i in the M_0 basis we have for $i=0,1$

$$M_{i,\pm}: c'_\pm = i(1-\lambda_\pm)+\lambda_\pm c_\pm , \tag{4}$$

Hence, in this representation the pair of 2D maps M_i reduces to two separate $(\pm)$ pairs of 1D maps $M_{i,\pm}$. Both $\pm$ trajectories are coded by the same stochastic map sequence. The eigenvalues $\lambda_\pm$ can be made to vary such that $0\le\lambda_-\le\lambda_+\le 1$. Therefore we now focus on the 1D case and to simplify the notation the branches f_i are defined by

$$f_i: x'_i = i(1-\lambda)+\lambda x \quad (i=0,1), \tag{5}$$

where the eigenvalue λ is the contraction parameter and x is the fractional distance along the corresponding side (eigendirection) of the parallelogram.

The branches of (5) define the stochastic difference equation

$$x(t+1)=\lambda x(t)+(1-\lambda)\xi(t), \tag{6}$$

where $\xi(t)$ is the Boolean random variable defined in (3). At any λ, the invariant density of the stochastic process (6) can be obtained from a single trajectory. Figure 1 shows the λ dependence of this density for $p=\frac{1}{2}$ in the λ-x plane. Evidently, the invariant density is organized by two infinite sets of lines that emerge from $x=0$ and $x=1$ at $\lambda=0$. Lines in one set only cross lines in the other, so for $\lambda<\frac{1}{2}$ there are no crossings giving a gap-filled structure. For $\lambda>\frac{1}{2}$ most of the interval is accessible; a conspicuous latticelike region of crossings near $\lambda=\frac{1}{2}$ changes abruptly, at $\lambda=(\sqrt{5}-1)/2$, into a region of smooth density at larger λ. We now discuss the distinctive behavior in these three regimes, and the singular behavior at the parameter points that separate them.

Cantor set regime.—For $\lambda\in(0,\frac{1}{2})$, the invariant density is a Cantor set. Under f_0 the interval [0,1] is mapped into $[0,\lambda]$, while under f_1 it is mapped into $[1-\lambda,1]$. For $\lambda<\frac{1}{2}$ these intervals are disjoint with an intervening gap. Successive iterations of the map produce a hierarchy of nested, disjoint intervals whose limit is a Cantor set with scaling length λ, so the fractal dimension[2] D is $-\log 2/\log\lambda$. At $\lambda=0$, $D=0$ because the Cantor set has collapsed onto the end points $x=0$ and $x=1$, and at $\lambda=\frac{1}{2}$, $D=1$ because it fills the unit interval.

Resonance regime.—For $\lambda\in[\frac{1}{2},(\sqrt{5}-1)/2]$, the crossing sets of lines produce self-similar bands in the invariant density. It is useful to consider the stationary solutions ρ^* to the Chapman-Kolmogorov equation corresponding to (6):

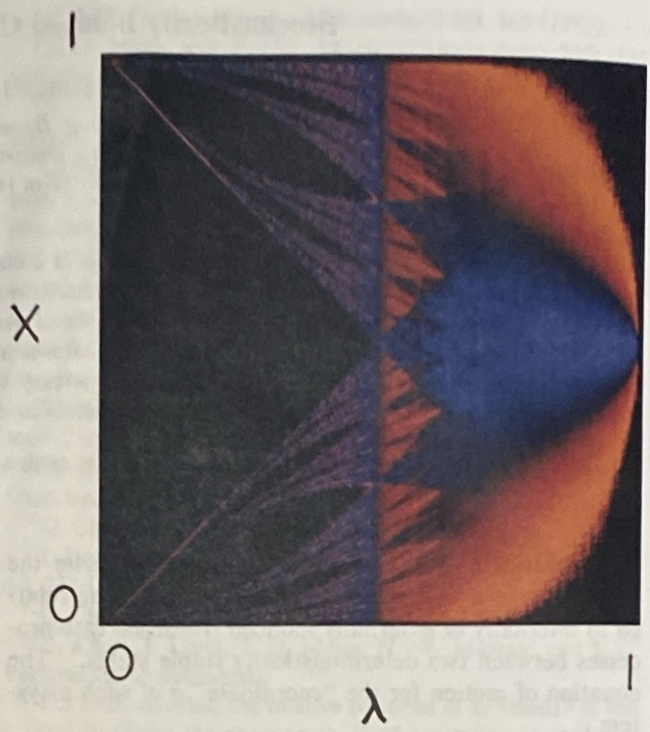

FIG. 1. Stationary density ρ^* in the λ-x plane. High-density regions are blue and low-density regions are red.

$$\rho(x,t+1)=\lambda^{-1}\{p\rho(x/\lambda,t)+(1-p)\rho((x+\lambda-1)/\lambda,t)\}, \tag{7}$$

which must be solved subject to the condition that $\rho^*(x)=0$ for $x\notin[0,1]$. The spectrum of (7) lies in the open unit disk, apart from eigenvalue 1 for ρ^*, so this stationary density can be found by iteration. However, we can also find ρ^* explicitly at some λ; e.g., at $\lambda=\frac{1}{2}$ where crossing first occurs the density is uniform for $p=\frac{1}{2}$.

For all values of $\lambda>\frac{1}{2}$ the support[2] of ρ^* is [0,1] (but ρ^* may vanish on a dense set). For λ just above $\frac{1}{2}$, Fig. 1 shows structured high-density (blue) wedges corresponding to flat-topped peaks; as λ increases these merge into regions of low-density (red) wedges which we term trough resonances. The most intense of these occurs at $\lambda=(\sqrt{5}-1)/2$. For larger λ there are only faint structures, and these seem to disappear above $\lambda=1/\sqrt{2}$. The origin of these resonances is not difficult to understand. We first examine the nature of the envelope of ρ^* near the end points 0 and 1. The integral of $\rho^*(x)$ over an interval $[0,x]$ is the distribution function or mass on that interval $m^*(0,x)$, say. For ρ^*, Eq. (7) then yields

$$m^*(0,x)=pm^*(0,x/\lambda)+(1-p)m^*(0,(x+\lambda-1)/\lambda). \tag{8}$$

If x is chosen such that $x<1-\lambda$, which is true suffi-

Fig. 1

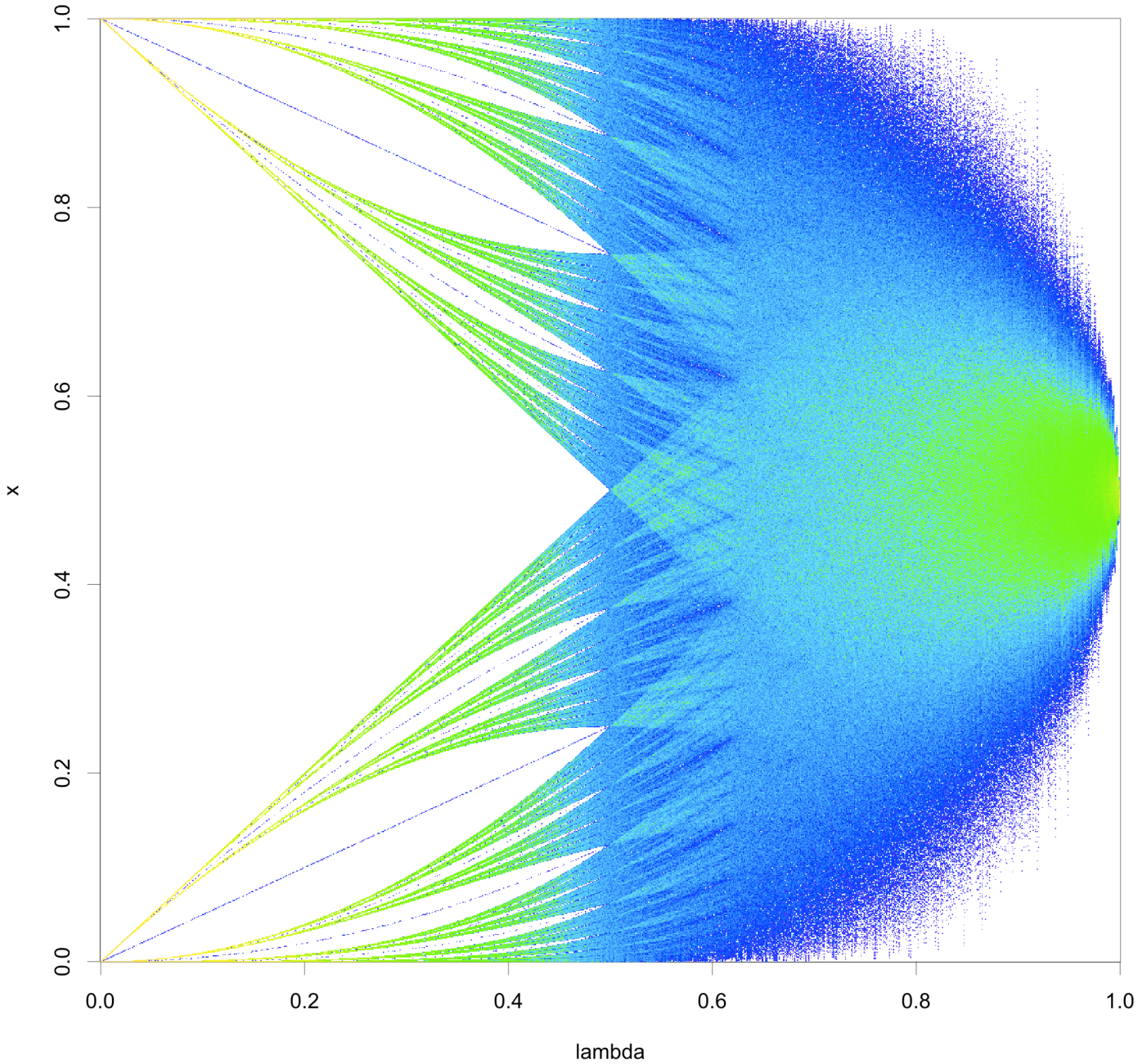

ciently close to the origin, the second term of (8) is zero and $m^*(0,x)=pm^*(0,x/\lambda)$. This equation admits a power-law solution $m^*(0,x)\sim x^{\nu_0}$, where $\nu_0=\log p/\log\lambda$. A similar analysis for the behavior near $x=1$ yields a power-law behavior with an exponent of $\nu_1=\log(1-p)/\log\lambda$. The envelope of ρ^* near the origin is given by the derivative of the probability mass and thus $\rho^*(x)\sim x^{z_0}$, with $z_0=\nu_0-1$. Consider the case $p=\frac{1}{2}$; for $\frac{1}{2}<\lambda<1/\sqrt{2}$, $0<z_0<1$, the density envelope goes to zero with infinite slope. This cusp behavior of the density near the origin (and near unity) is responsible for the trough resonances as can be seen from the following argument.

The resonances arise from the existence of periodic orbits which contain two points that are (finite) images of 0 under f_1 and 1 under f_0, respectively, i.e., eventually periodic orbits. Consider the family of periodic orbits with two points on the orbit arising from *first* images of 0 and 1 as described above. For $p=\frac{1}{2}$ the periodic orbits possess a mirror symmetry under the f_0 and f_1 maps so that a period-$2n$ orbit consists of n steps to the left on f_0 and n steps to the right on f_1. The condition for the existence of such a period-$2n$ orbit is easily written as

$$f_0\circ f_1^{(n-1)}\circ f_0(1)=f_1(0)\,, \tag{9}$$

where $f_i^{(n)}$ is the nth composition of the map. An equivalent representation of the periodic orbit can be obtained from (9) by the replacement $0\leftrightarrow 1$. Since these periodic orbits contain points which are images of 0 and 1, and the density goes to zero as a power law at these points, then this cusp behavior is replicated at all points of the periodic orbit. Since the number of these images doubles under the two branches of the map, the invariant density vanishes on the uncountable limit set of these cusped zeros.

The simplest periodic orbit of this type has period 2, and for this case (9) reduces to $p_1(\lambda)\equiv\lambda^2+\lambda-1=0$, whose solution is the golden mean $\lambda_1=(\sqrt{5}-1)/2$. Figure 2 shows the invariant density corresponding to this golden-mean resonance.[3] Note the large troughs at x equal to λ and $1-\lambda$, the images of 1 and 0 under f_0 and f_1, respectively. The remaining troughs arise from higher-order images as described above. The λ values corresponding to the "daughters" of this resonance can be constructed in a similar way from (9) for $n=2,3,\ldots$. In fact, it is not difficult to show that a simple scaling relation exists for this family of periodic orbits. If we let $p_n(\lambda)$ denote the polynomial[4] that results from (9) for a period-$2n$ orbit, we have the following recursion relation:

$$p_{n+1}(\lambda)=\lambda p_n(\lambda)+(1-\lambda)(2\lambda-1)\,. \tag{10}$$

The fixed-point function of this equation $p^*(\lambda)$ gives the value of λ_∞ corresponding to the "root" of this first family tree. We find $p^*(\lambda)=2\lambda-1$ or $\lambda_\infty=\frac{1}{2}$, where $\rho^*=1$ for $x\in[0,1]$ and is zero elsewhere, i.e., it is piecewise smooth. The asymptotic scaling relation for λ easily follows from (10). Letting $\lambda_n=\lambda_\infty+\delta\lambda_n$ we have $\delta\lambda_{n+1}=\frac{1}{2}\delta\lambda_n$ (geometric convergence) for large n. As one progresses through the family tree, starting with the golden-mean resonance, the orbits increase in length until at the root we have a symmetric infinite-period orbit. Other resonance family trees can be constructed in the same way, and should show the same generic features.

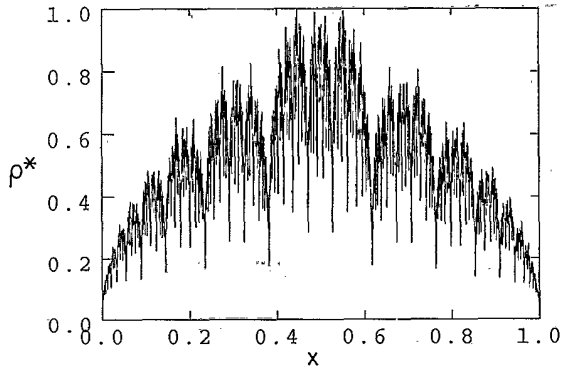

FIG. 2. Density ρ^* vs x for strong resonance at $\lambda_1=(\sqrt{5}-1)/2$.

Smooth density regime.—The value $\lambda=1/\sqrt{2}$ signals a change in the behavior of the density envelope near 0 and 1 for $p=\frac{1}{2}$. In this case the exponent $z_0=1$ and $\rho(x)\sim x$ near $x=0$; the density goes linearly to zero at the end points 0 and 1. If $\lambda>1/\sqrt{2}$ then $z_0>1$ and $\rho(0)=\rho'(0)=0$ and the density goes smoothly to zero as a power law. So while periodic orbits of the type discussed above may be constructed, the absence of cusplike behavior near the end points gives rise to an apparently smooth invariant density.

If the dynamics is not overdamped as assumed above the full 2D map, (3) must be studied and an even richer structure for the invariant density exists. In the underdamped regime the decay is oscillatory, which gives rise to a spiral structure for the invariant density in the (q,v) plane with self-similar features.

It should be possible to observe stochastically induced coherence in bistable systems subjected to periodic dichotomous noise processes that produce hops between the bistable states. We describe a few specific examples here. The iodate-arsenous acid reaction may be carried out in a continuous-flow stirred tank reactor under far-from-equilibrium conditions.[5] If arsenous acid is in excess, a detailed consideration of the reaction mechanism shows that the iodide-ion concentration $x=[I^-]$ satisfies a cubic-rate law, $\dot{x}=-ax^3+bx^2-cx+d$, where a, b, c, and d are parameters that depend on the chemical rate constants and feed concentrations.[5] The cubic kinetics correspond to an underlying quartic "potential" function and bistable steady states exist for a range of parameter values. The parameter d may be made a periodic dichotomous random variable by randomly switching the iodide and iodate ($[I^-]_0$ and $[IO_3^-]_0$) input feeds to the

reactor.[6] The input feeds can be switched on a time scale of 1–5 sec while the characteristic relaxation time for hops between the bistable states is 2–5 min. Thus in a typical experimental run of 20 h, approximately 500–1000 observations can be made which corresponds to roughly ten Cantor set decimations in the invariant density.[7]

Optical bistable devices are good candidates for experimental studies because of the shorter time scales involved in their operation (hop relaxation times can vary from 100 μsec to a few msec).[8] Under some conditions (a quantity proportional to) the output intensity of the Ikeda or hybrid optical bistable devices[9] satisfies a nonlinear mapping equation with a sinusoidal nonlinearity. The input intensity is a convenient bifurcation parameter and the system displays a prominent region of bistability between steady states.[9] The local dynamics in the vicinity of this bistability corresponds to motion in a bistable potential and the input laser intensity can be made a periodic dichotomous noise process to induce hops between the two output states of the nonlinear optical device. Recently,[10] an optical bistable device that can be switched from clockwise to counterclockwise lasing operation was used to study stochastic resonance. By modifying the way the frequency of the acousto-optic modulator is changed to correspond to periodic dichotomous switching and by changing the operating conditions of the laser so that the lasing direction switches even in the absence of the additional external noise required for stochastic resonance, one may construct an optical device for the observation of stochastically induced coherence.

The principle features needed for the observation of the effects described in this paper are a bistable system that can be forced with a periodic dichotomous noise process to effect hops between the bistable states. Thus we expect the phenomenon to be generally observable in a broad class of systems of this type.

This research was supported in part by grants from the Natural Sciences and Engineering Research Council of Canada (R.K. and S.J.E.) and the Petroleum Research Fund administered by the American Chemical Society (R.K.). We would like to thank Tim Bedford and Jean-Pierre Kahane for helpful conversations.

[1]See, e.g., *Noise in Nonlinear Dynamical Systems,* edited by F. Moss and P. V. E. McClintock (Cambridge Univ. Press, Cambridge, 1989).

[2]K. J. Falconer, *The Geometry of Fractal Sets* (Cambridge Univ. Press, Cambridge, 1984).

[3]P. Erdös, Am. J. Math. **61**, 974 (1939).

[4]The significant root ($\lambda \in [0,1]$) of any $p_n(\lambda)$ is a reciprocal Pisot-Vijayaraghavan number. See C. Pisot, Ann. Pisa **7**, 205 (1938); T. Vijayaraghavan, Proc. Cambridge Philos. Soc. **37**, 349 (1941).

[5]A. Saul and K. Showalter, in *Oscillations and Traveling Waves in Chemical Systems,* edited by R. J. Field and M. Burger (Wiley, New York, 1985).

[6]I. L'Heureux and R. Kapral, J. Chem. Phys. **88**, 7468 (1988).

[7]The externally forced iodate-arsenous acid system is being studied by J. P. Laplante, Royal Military College, and we thank him for the time-scale estimates given in the text.

[8]K. Ikeda, Opt. Commun. **30**, 257 (1979); F. A. Hopf, D. L. Kaplan, H. M. Gibbs, and R. L. Shoemaker, Phys. Rev. A **25**, 2172 (1982).

[9]B. McNamara, K. Weisenfeld, and R. Roy, Phys. Rev. Lett. **60**, 2626 (1988).

[10]R. Benzi, A. Sutera, and A. Vulpiani, J. Phys. A **14**, L453 (1981).